chemistry proceedings

MDPI

Proceeding Paper

Participation of the Cyanide Group in the Reaction Mechanism of Benzoxazole Formation: Monitoring by Continuous Flow Cell NMR †

Nelda Xanath Martínez-Galero [1,*], Daniel Galindo [2], Lemuel Pérez-Picaso [1] and Lucio Peña-Zarate [2,*]

[1] Organic Synthesis Laboratory, Scientific Research Center, Applied Chemistry Institute, Universidad del Papaloapan, Tuxtepec, Oaxaca 68301, Mexico; email1@email.com
[2] Organic Synthesis Laboratory, Licenciatura en Ciencias Químicas, Universidad del Papaloapan, Tuxtepec, Oaxaca 68301, Mexico; lucio.pena@cinvestav.mx
* Correspondence: nmartinez@unpa.edu.mx (N.X.M.-G.); lucio.pena@cinvestav.mx (L.P.-Z.); Tel.: +52-2878759240 (e230)
† Presented at the 29th International Electronic Conference on Synthetic Organic Chemistry (ECSOC-29); Available online: https://sciforum.net/event/ecsoc-29.

Abstract

Benzoxazoles are recognized as significant building blocks in organic synthesis and materials science. This work observed the formation of benzoxazole from o-aminophenol and o-hydroxybenzaldehyde using online ^{1}H NMR (continuous flow cell, 80 MHz). The identification of changes in the functional group was complemented by ATR-FTIR analysis. Additionally, the kinetic roles of phenylboronic acid and cyanide in the one-pot condensation-cyclization reaction are examined. Real-time monitoring has revealed three observable events: the rapid condensation of the aldehyde and o-aminophenol to produce the imine; the formation of the boron complex in the presence of phenylboronic acid; and the cyanide-assisted cyclization that converts the intermediate into benzoxazole. The findings clarify the transformations that control throughput and provide valuable insights for optimizing reagent loadings under environmentally friendly conditions.

Keywords: monitoring reactions; kinetics of reactions; one-pot synthesis

Academic Editor(s): Name

Published: date

Citation: Martínez-Galero, N.X.; Galindo, D.; Pérez-Picaso, L.; Peña-Zarate, L. Participation of the Cyanide Group in the Reaction Mechanism of Benzoxazole Formation: Monitoring by Continuous Flow Cell NMR. *Chem. Proc.* **2025**, *volume number*, x. https://doi.org/10.3390/xxxxx

1. Introduction

In catalyzed reactions, catalysts accelerate a desired transformation by lowering the activation barrier and biasing pathway selection among competing channels. Promoters are distinct from catalysts in that they typically exhibit negligible turnover in isolation but enhance the performance of a catalyst, for example, by tuning the electronic environment, adsorption thermodynamics, or transport to the active site; the effect can manifest as higher activity, altered selectivity, or improved catalyst stability [1]. When catalysts and promoters are used together, synergistic effects often occur. This means that there can be changes in the rate constants of elementary steps, the thermodynamic equilibria of intermediates, or the kinetic partitioning between different mechanistic pathways. Therefore, understanding the mechanisms of reactions requires careful analysis to find which steps are controlled by kinetics, which are influenced by thermodynamics (pre-equilibrium), and where phenomena such as saturation or inhibition might arise [2].

Otherwise, benzoxazoles are versatile heteroaromatic compounds in medicinal and materials chemistry [3–9]. Various protocols involve the condensation of aldehydes with o-aminophenols followed by oxidative cyclization and dehydration under mild conditions, including metal-free, metal-catalyzed, and promoter-assisted variations [10–19].

Despite the rich method literature, the relative kinetic roles of (i) imine formation (condensation), (ii) boron complexation (such as phenylboronic acid as promoter, and considering published evidence on the boron complex formed between phenylboronic acid and the imine) [16–18], and (iii) cyanide-enabled aerobic cyclization have not been consistently analyzed under either batch or flow conditions [20,21]. In this study, we utilize benchtop 1H NMR [22–26], with online flow cell [27–29], supplemented by ATR-FTIR, to achieve: (i) determine the kinetic order of the condensation step (imine formation), (ii) investigate whether boron complexation influences the reaction rate (for example, by altering equilibrium or stabilizing the transition state), and (iii) assess how the cyclization step (forming benzoxazole) depends on the concentration of cyanide.

2. Materials and Methods

Reagents. Salicylaldehyde (**1**), 2-aminophenol (**2**), phenylboronic acid (PBA), and KCN were used as received (≥99%). Deuterated NMR solvents: MeOD, $CDCl_3$, DMSO-d_6; TMS as internal standard. Reagents and solvents were obtained from Sigma Aldrich.

All reactions were carried out under ambient temperature (≈ 25 °C) and pressure in a 10.0 mL total volume with the following stoichiometry: 1.0 equiv of **1** and **2**; PBA at 0.1, 0.5, or 1.0 mol %; KCN at 0.5, 1.0, or 1.5 equiv. PBA was dissolved in minimal MeOH and KCN in minimal H_2O, and then the two solutions were combined. The PBA content and water activity are mechanistically relevant because boronic acids form boroxines and boronate esters in dynamic equilibria that influence dehydration.

A benchtop NMR (Magritek, Spinsolve 80 MHz) with a continuous flow cell acquired ^{1}H NMR spectra every 5 min without interrupting flow. ATR FTIR (PerkinElmer, Spectrum 100) tracked C=O, C=N, and O–H bands to support assignments. Typical ^{1}H NMR handles: aldehydic CHO (~10 ppm), imine CH (~9 ppm), and diagnostic aromatic resonances of benzoxazole **4** (~8 ppm). Evidence indicates the formation of boron-complex **A** from imine **3** and the subsequent formation of benzoxazole **4** (Figure 1) [16].

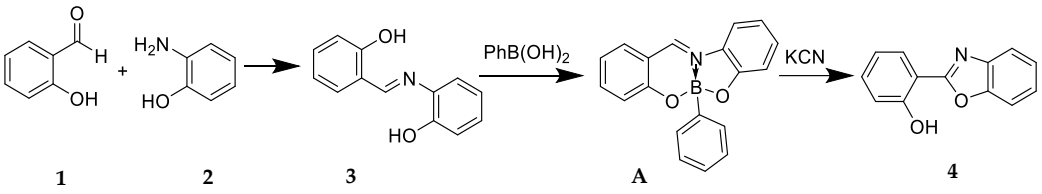

Figure 1. Synthesis of 2-arylbenzoxazole **4**, promoted by PBA and KCN [16].

Rate orders were obtained by initial rate analysis from early, linear regime data while varying the initial concentration of a single component at constant others, and integrated rate fitting to appropriate forms. The influence of PBA was tested by varying its loading at fixed substrate concentrations. Cyanide dependence was examined by varying KCN while holding other parameters constant. All measurements were performed in replicate; fits were evaluated by residual inspection and goodness of fit metrics.

3. Results and Discussion

The initial-rate analysis and integrated fits indicate that the condensation step follows a second-order rate law, being first-order in both aldehyde and aminophenol. In contrast, the rate of boron complex formation appears to be independent of the concentration of

PBA within the ranges examined. Lastly, the step involving cyanide addition shows zero-order behavior with respect to benzoxazole, suggesting that the cyanide concentration does not influence the rate-limiting step under these conditions. This could indicate that a cyanide-dependent pre-equilibrium is saturated. Figure 2 illustrates the kinetic behavior of the reaction conducted in a continuous flow cell with online NMR in methanol (MeOH). In part (a), the red line represents the rate of aldehydic proton consumption, while the yellow line indicates the rate of imine formation. In part (b), the red line shows the rate of imine consumption, and the yellow line represents the rate of benzoxazole formation.

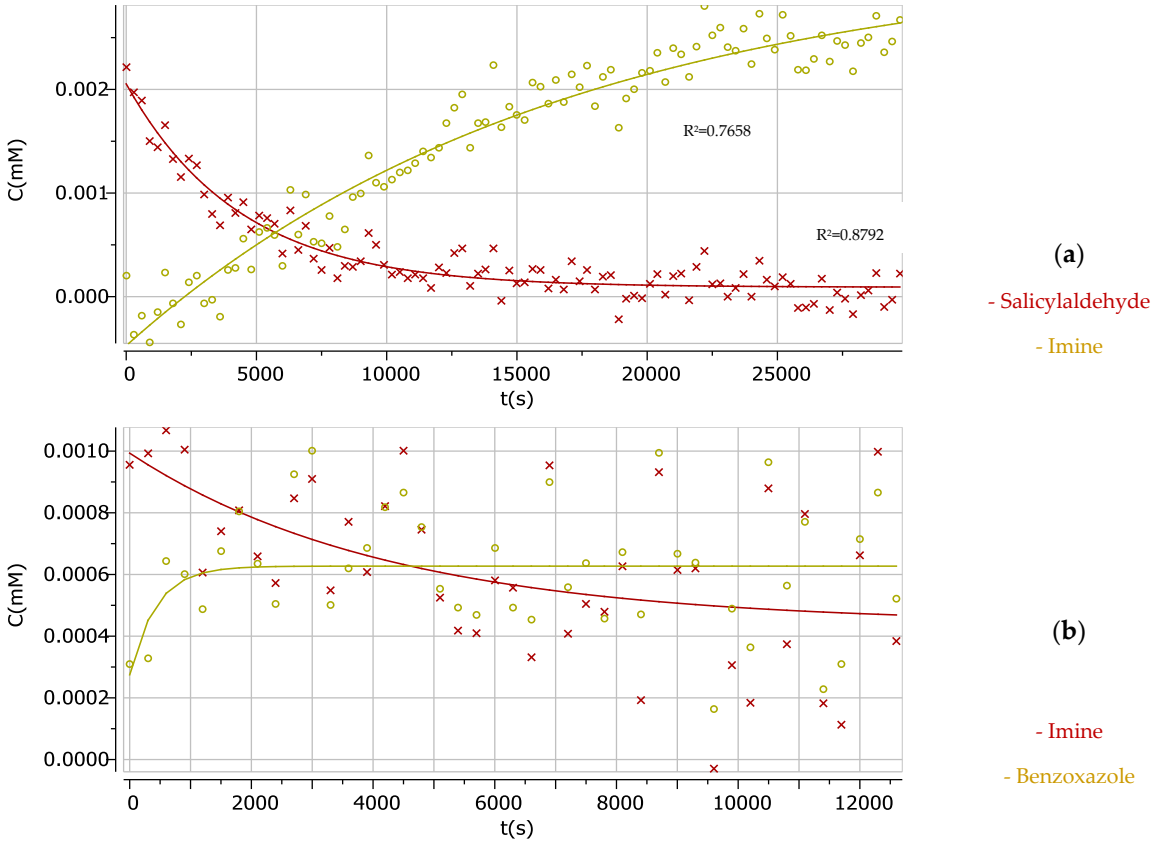

Figure 2. Reaction kinetics using a continuous flow cell in an online NMR in MeOH: (**a**) Rate of aldehydic proton consumption (red line) and imine formation (yellow line); (**b**) Rate of imine consumption (red line) and benzoxazole formation (yellow line).

The rapid second-order reaction in the condensation step follows a classic mechanism. This involves a nucleophilic attack of aminophenol **2** on the aldehyde carbonyl **1**, leading to the formation of a hemiaminal, which is then dehydrated. Afterward, the data indicate that the yield is controlled during the intermediate phase by boron complex **A** formation. In the final phase, while cyanide promotes oxidative cyclization, the formation of benzoxazole **4** occurs in a zero-order reaction. This means that the concentration of benzoxazole remains constant over time and is independent of the amount of cyanide used (0.5, 1.0, and 1.5 equivalents).

Together, these data indicate that throughput is controlled upstream by the bimolecular condensation, not by downstream borate or cyanide events. The second-order dependence in the condensation step aligns with a classical pathway (nucleophilic attack of the aminophenol on the aldehyde to give a hemiaminal, followed by dehydration). The borate complex is readily detected but kinetically innocent under our conditions, consistent with an off-cycle or fast equilibrium role that does not limit flux to product. Finally, zero-order behavior in CN^- rules out CN participation in the rate-determining transition

state (within the tested domain), or indicates that CN-dependent activation is saturated, making subsequent, CN-independent chemistry rate-limiting. The proposal mechanistic pathway (Figure 3) begins with condensation (imine formation) to give intermediate **3**, followed by reversible complexation with PBA to yield boron-complex **A**, and finally cyanide-promoted oxidative cyclization to benzoxazole **4**.

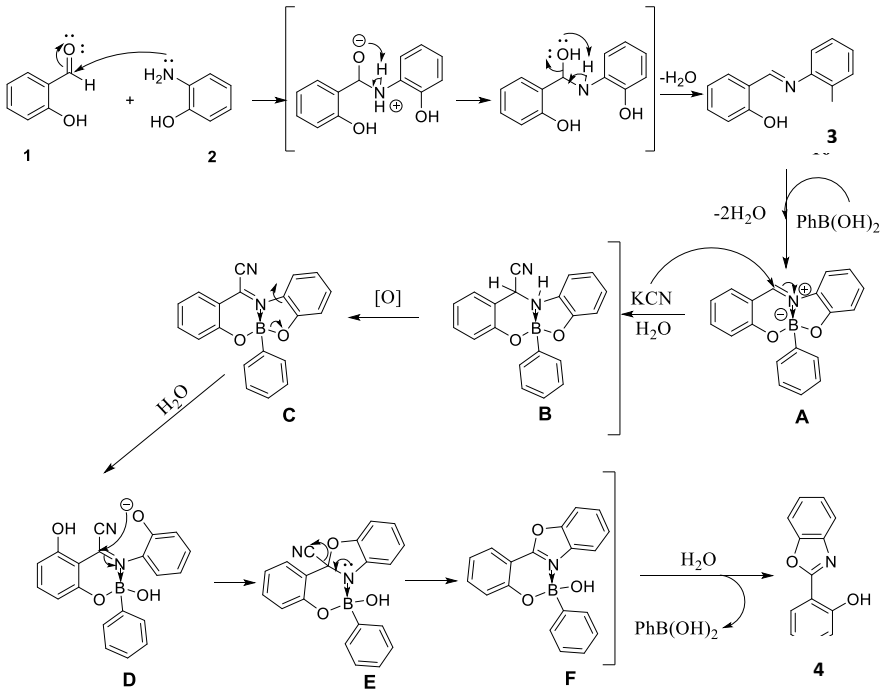

Figure 3. Proposed pathway: By condensation to form imine **3**, then through complexation with PBA to form boron complex **A**. Finally, the rate-determining step, cyanide-mediated cyclization to produce **4**.

Practical implications: to accelerate the process, increasing either aldehyde or aminophenol concentration is effective (bimolecular control), whereas increasing boron or cyanide is not; catalyst choice may be guided toward promoters that accelerate condensation, rather than downstream cyclization; the kinetic neutrality of boron and cyanide under these conditions suggests scope to lower their loadings without throughput penalties, improving process mass intensity.

Author Contributions: N.X.M.-G.: Conceptualization, methodology, resources, supervision, project administration. L.P.-Z.: writing—original draft preparation, visualization, software, validation, formal analysis. N.X.M.-G.; D.G., L.P.-P. and L.P.-Z.: writing—review and editing, investigation. All authors have read and agreed to the published version of the manuscript. Authorship must be limited to those who have contributed substantially to the work reported.

Funding: This research received no external funding.

Institutional Review Board Statement: Not applicable.

Informed Consent Statement: Not applicable.

Data Availability Statement:

Conflicts of Interest: The authors declare no conflicts of interest.

Appendix A

Appendix A.1

The kinetics of the reaction between compound **1** and compound **2**, leading to the formation of the imine intermediate 3, were studied. In the subsequent ^{1}H NMR spectrum, a decrease in the intensity of the signal corresponding to the aromatic aldehyde proton at 9.77 ppm (a), was observed over the acquisition time of the spectra. Conversely, the signal for the imine at 8.64 ppm increased in intensity (b). Additionally, a cluster of multiple signals observed between 7.5 and 6.9 ppm corresponds to the protons of the aromatic groups. Representative stacked NMR spectra of the monitored reactions. The spectra were collected every 5 min during the online reaction time.

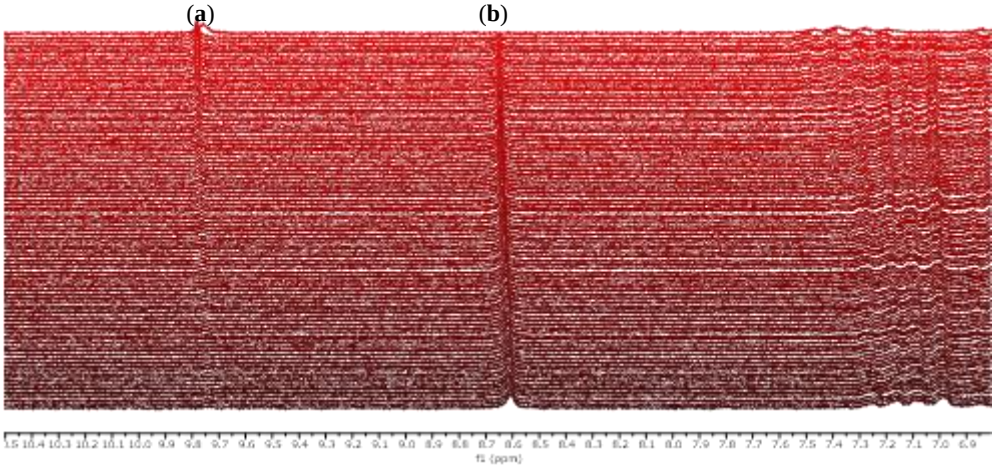

Figure A1. ^{1}H NMR spectra of the reaction monitoring: (**a**) the proton signal of the aromatic aldehyde at 9.77 ppm and (**b**) the proton signal of the imino group in the intermediate at 8.64 ppm.

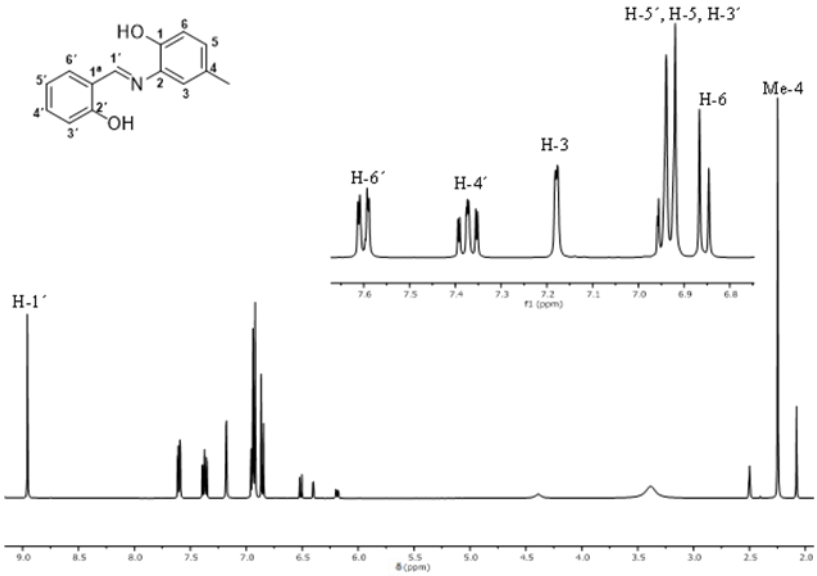

Figure A2. ^{1}H NMR spectra of imino intermediate 1a-[[(2-hydroxy-4-methylphenyl) imino]methyl]phenol **3**.

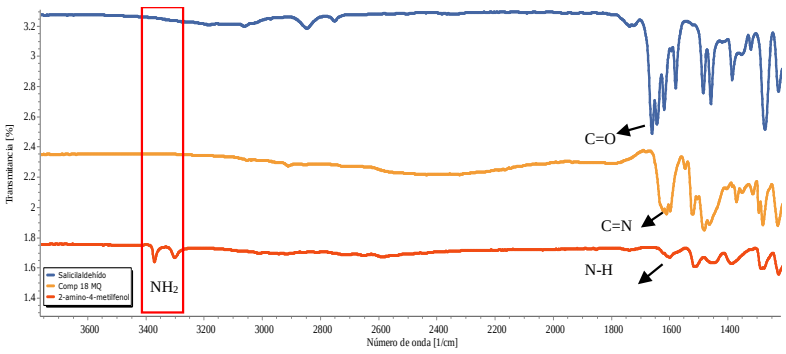

Figure A3. Stacked FTIR-ATR spectra of salicylaldehyde **1** (blue), imine **3** (yellow), and 2-amino-4-methylphenol **2** (orange).

References

1. Horáček, J. Fischer–Tropsch synthesis, the effect of promoters, catalyst support, and reaction conditions selection. *Monatsh. Chem.* **2020**, *151*, 649–675.
2. Meek, S.J.; Pitman, C.L.; Miller, A.J.M. Deducing reaction mechanism: A guide for students, researchers, and instructors. *J. Chem. Educ*. **2016**, *93*, 275–286.
3. Sun, L.; Wang, X.; Fleurat-Lessard, P.; Gros, C.P.; Bolze, F.; Xu, H. Synthesis, photophysical properties and two-photon absorption of benzothiazole/benzoxazole π-expanded carbazole dyes. *Dyes Pigment.* **2022**, *204*, 110447.
4. Bremond, E.; Leygue, N.; Saffon-Merceron, N.; Fery-Forgues, S. 2-Phenylbenzoxazole derivatives as solid-state fluorescence emitters: Influence of steric hindrance and hydrogen bonding on the optical properties. *Spectrochim. Acta Part A Mol. Biomol. Spectrosc.* **2020**, *227*, 117586.
5. Carayon, C.; Fery-Forgues, S. 2-Phenylbenzoxazole derivatives: A family of robust emitters of solid-state fluorescence. *Photochem. Photobiol. Sci.* **2017**, *16*, 1020–1035.
6. Vetrova, E.V.; Tupaeva, I.O.; Sayapin, Y.A.; Gusakov, E.A.; Nikolaevskii, S.A.; Demidov, O.P.; Minkin, V.I.; Metelitsa, A.V. Chromogenic properties of 2-(2-carbomethoxy-3,4-dichloro-6-hydroxyphenyl)benzoxazole and its Zn(II) and Cd(II) complexes. *Dyes Pigment.* **2020**, *180*, 108417.
7. Wang, J.; Baumann, H.; Bi, X.; Shriver, L.P.; Zhang, Z.; Pang, Y. Efficient synthesis of NIR emitting bis [2-(2′-hydroxylphenyl)benzoxazole] derivative and its potential for imaging applications. *Bioorganic Chem.* **2020**, *96*, 103585.
8. Wei, P.-F.; Qi, M.-Z.; Wang, Z.-P.; Ding, S.-Y.; Yu, W.; Liu, Q.; Wang, L.-K.; Wang, H.-Z.; An, W.-K.; Wang, W. Benzoxazole-linked ultrastable covalent organic frameworks for photocatalysis. *J. Am. Chem. Soc.* **2018**, *140*, 4623–4631.
9. Pathak, A.; Thomas, K.R.J.; Singh, M.; Jou, J.H. Fine tuning of photophysical and electroluminescence properties of benzoxazole based dyes. *J. Org. Chem.* **2017**, *82*, 12188–12200.
10. Kawashita, Y.; Nakamichi, N.; Kawabata, H.; Hayashi, M. Direct and practical synthesis of 2-arylbenzoxazoles promoted by activated carbon. *Org. Lett.* **2003**, *5*, 3713–3715.
11. Wu, M.; Hu, X.; Liu, J.; Liao, Y.; Deng, G.J. Iron catalyzed 2-arylbenzoxazole formation from o-aminophenols and aldehydes. *Org. Lett.* **2012**, *14*, 5306–5309.
12. Nguyen, X.T.T.; Nguyen, T.T.; Nguyen, H.L.H.; Tran, P.H. Synthesis of benzoxazoles, benzimidazoles, and benzothiazoles Using a Brønsted acidic ionic liquid gel. *ACS Omega* **2019**, *4*, 21999–22008.
13. Soni, S.; Sahiba, N.; Teli, S.; Teli, P.; Agarwal, L.K.; Agarwal, S. Advances in the synthetic strategies of benzoxazoles using 2-aminophenol as a precursor: An up to up-to-date review. *RSC Adv*. **2023**, *13*, 24358–24391.
14. Liu, Y.; Mao, D.; Lou, S.; Qian, J.; Xu, Z. Facile and efficient one pot synthesis of 2-arylbenzoxazoles catalyzed by HAuCl4. *J. Zhejiang Univ. Sci. B* **2009**, *10*, 629–633.
15. Naeimi, H.; Rouzegar, Z.; Rahmatinejad, S. Catalyst-free microwave-promoted one pot synthesis of 2-aryl benzoxazoles using MnO_2 nanoparticles as a convenient oxidant under mild condition. *Res. Chem. Intermed.* **2017**, *43*, 4745–4758.
16. López Ruiz, H.; Briseño Ortega, H.; Rojas Lima, S.; Santillán, R.; Farfán, N. An efficient potassium cyanide promoted synthesis of 2 Arylbenzoxazoles from [4.3.0] boron heterobicycles. *Tetrahedron Lett.* **2010**, *51*, 2633–2635.
17. Reyes, H.; Beltran, H.I.; Rivera Becerril, E. One pot synthesis of 2 phenylbenzoxazoles by potassium cyanide assisted reaction of o-aminophenols and benzaldehydes. *Tetrahedron Lett*. **2011**, *52*, 308–310.

18. López Ruiz, H.; Briseño Ortega, H.; Rojas Lima, S.; Santillán, R.; Farfán, N. Phenylboronic acid catalyzed, cyanide promoted one pot synthesis of 2 (2 Hydroxyphenyl)benzoxazoles. *Tetrahedron Lett.* **2011**, *52*, 4308–4312.
19. Peña-Zarate, L. Mecanosíntesis de benzoxazoles funcionalizados con potencial aplicación en el desarrollo de diodos orgánicos emisores de luz. Bachelor's Thesis, Universidad del Papaloapan, Oaxaca, Mexico, 17 September 2020.
20. Doan, S.H.; Tran, C.B.; Cao, A.L.N.; Le, N.T.H.; Phan, N.T.S. A new pathway to 2-arylbenzoxazoles and 2-arylbenzothiazoles via one-pot oxidative cyclization reactions under iron-organic framework catalysis. *Catal. Lett.* **2019**, *149*, 2053–2063.
21. Henry, M.C.; Abbinante, V.M.; Sutherland, A. Iron-catalyzed regioselective synthesis of 2-arylbenzoxazoles and 2-arylbenzothiazoles via alternative reaction pathways. *Eur. J. Org. Chem.* **2020**, *19*, 2819–2826.
22. Kircher, R.; Mross, S.; Hasse, H.; Münnemann, K. ^{1}H Benchtop NMR Spectroscopy by paramagnetic shift reagents for process monitoring. *Appl. Magn. Reson*. **2023**, *54*, 1515–1532.
23. Ji, Y.; Lin, Z.; Lawon, L.; Lévesque, F.; Foley, D.A.; Espina, R.; Robert, H. Coupling probe based autosampler with Benchtop NMR for automated sampling and online measurement. *React. Chem. Eng*. **2023**, *8*, 3323–3331.
24. Giberson, J.; Scicluna, J.; Legge, N.; Longstaffe, J. Developments in Benchtop NMR Spectroscopy 2015–2020. *Prog. Nucl. Magn. Reson. Spectrosc.* **2021**, *124–125*, 1–28.
25. Kern, S.; Wander, L.; Meyer, K.; Guhl, S.; Mukkula, A.R.G.; Holtkamp, M.; Salge, M.; Fleischer, C.; Weber, N.; King, R.; et al. Flexible automation with compact NMR for process analytics. *Anal. Bioanal. Chem.* **2019**, *411*, 5129–5141.
26. Burkhardtsmaier, P.; Pavlovskaja, K.; Maier, D.; Schäfer, S.; Salat, U.; Schmidt, M.S. Quantitative monitoring of fermentation by Benchtop NMR. *Food Anal. Methods* **2021**, *14*, 2369–2380.
27. Foley, D.A.; Bez, E.; Codina, A.; Colson, K.L.; Fey, M.; Krull, R.; Piroli, D.; Zell, M.T.; Marquez, B.L. NMR flow tube for Online NMR reaction monitoring. *Anal. Chem*. **2014**, *86*, 12008–12013.
28. Chae, Y.; Min, S.; Park, E.; Lim, C.; Cheon, C.H.; Jeong, K.; Kwak, K.; Cho, M. Real time reaction monitoring with in operando flow NMR and FTIR: Reaction mechanism of benzoxazole synthesis. *Anal. Chem*. **2021**, *93*, 2106–2113.
29. Gómez, M.V.; de la Hoz, A. NMR reaction monitoring in flow synthesis (Review). *Beilstein J. Org. Chem*. **2017**, *13*, 285–300.